Development of the Commercial Route for the Manufacture of a 5-Lipoxygenase Inhibitor PF-04191834

Brian Chekal, David Damon, Danny LaFrance, Kyle Leeman, Carlos Mojica, Andrew Palm, Michael St. Pierre, Janice Sieser, Karen Sutherland, Rajappa Vaidyanathan, John Van Alsten, Brian Vanderplas, Carrie Wager, Gerald Weisenburger, Gregory Withbroe, and Shu Yu*

Chemical Research and Development, Pfizer Worldwide R&D-Groton Laboratories, 558 Eastern Point Road, Groton, CT 06340, United States

Abstract:

A *de novo* three-step-one-pot process for the formation of **PF-04191834** was developed. This methodology employed inexpensive, odorless and readily available commodity chemical iso-octyl-3-mercaptopropionate as sulfur source, which could be a general alternative to the popular TIPS-SH in the formation of diarylthioethers via Migita coupling. A kinetic study revealed that at high temperature, reductive elimination could be the rate-limiting step in the catalytic cycle, which opens pathways for the generation of undesired impurities. By proper control of the reaction conditions, the desired API was synthesized in >70% crude yield and in 55% isolated yield after vigorous purifications. This process was successfully demonstrated on 20 kg scale.

Introduction

PF-04191834 (**1**), a potent competitive inhibitor of the 5-lipoxygenase (5 LOX) enzyme, has been explored as a treatment for mild to moderate asthma (Figure 1).[1,2] Based on projections of a high efficacious dose, it was expected that high volumes of API (**1**) would be required during both the clinical phase as well as commercially. In order to meet the expected demand, a more efficient and cost effective synthesis of **1** was required. This high volume posed an added challenge to the development of the commercial manufacturing process. In addition to ensuring the high quality of the API, considering the competitive nature of the asthma market, the commercial viability of this inhibitor also hinged on the cost of goods. Thus, in order to support

Phase 2 clinical trials and beyond, we required a highly cost-effective process for the manufacture of **PF-04191834** (**1**).

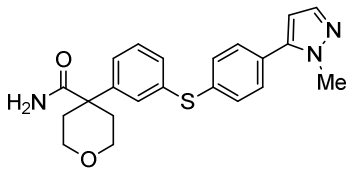

PF-04191834 (1)

Figure 1 Structure of 5-lipoxygenase inhibitor **PF-04191834 (1)**

The medicinal chemistry team designed a highly convergent route to **PF-04191834** (**1**) which was later enabled into an effective fit-for-purpose process for the manufacture of API for Phase 1 clinical trials (Scheme 1).[3] This route offered several advantages: a convergent synthesis with two raw materials of similar complexity (i.e., **2** and **5**), crystalline late-stage intermediates, chemistry involving mostly readily available reagents while avoiding extreme temperatures (low or high) and special equipment (such as high pressure and cryogenic conditions), and good to excellent yields for synthetic steps. Importantly, the two advanced intermediates, aryl bromides **2** and **5**, are both well-behaved, stable, highly-crystalline solids which could be sourced on multi-ton scale in reasonable time.

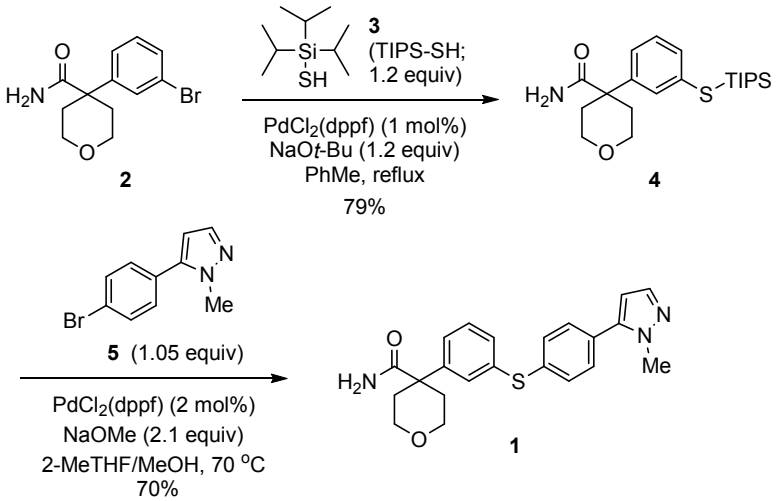

Scheme 1 First-generation synthesis of **PF-04191834** (**1**)

Further evaluation of the enabled chemistry revealed two major shortcomings that must be addressed. The first one is the narrow optimum operating range of the second Migita coupling. Under the reaction conditions, symmetrical sulfides **6** and **7** form readily (up to several percent, see Scheme 2), of which, **7** could not be purged by crystallization and could only be removed by chromatography. Since the impurities are the result of an unwanted reaction of the desired product, their formation increased as the reaction proceeded. In order to manage the level of symmetrical sulfides **6** and **7**, the reaction required the charge of the catalyst at 70 °C and stop within three hours. The fact that the API is not the most stable thermodynamic product in this transformation posed high challenge and risk on robustness and the quality assurance of the product.

The other one is the availability of the sulfur source for the first of two Migita couplings.[4] Triisopropylsilanethiol (**3**, TIPS-SH) is a versatile sulfur source that has been employed extensively in academia as well as medicinal chemistry.[5] However, its availability on scale is limited and only a single vendor was able to provide it on multikilogram scale at time this work was performed for a relatively high price. In addition, the reagent has a pungent rotten egg odor, which is an environmental risk. Therefore we sought an alternative sulfur source.

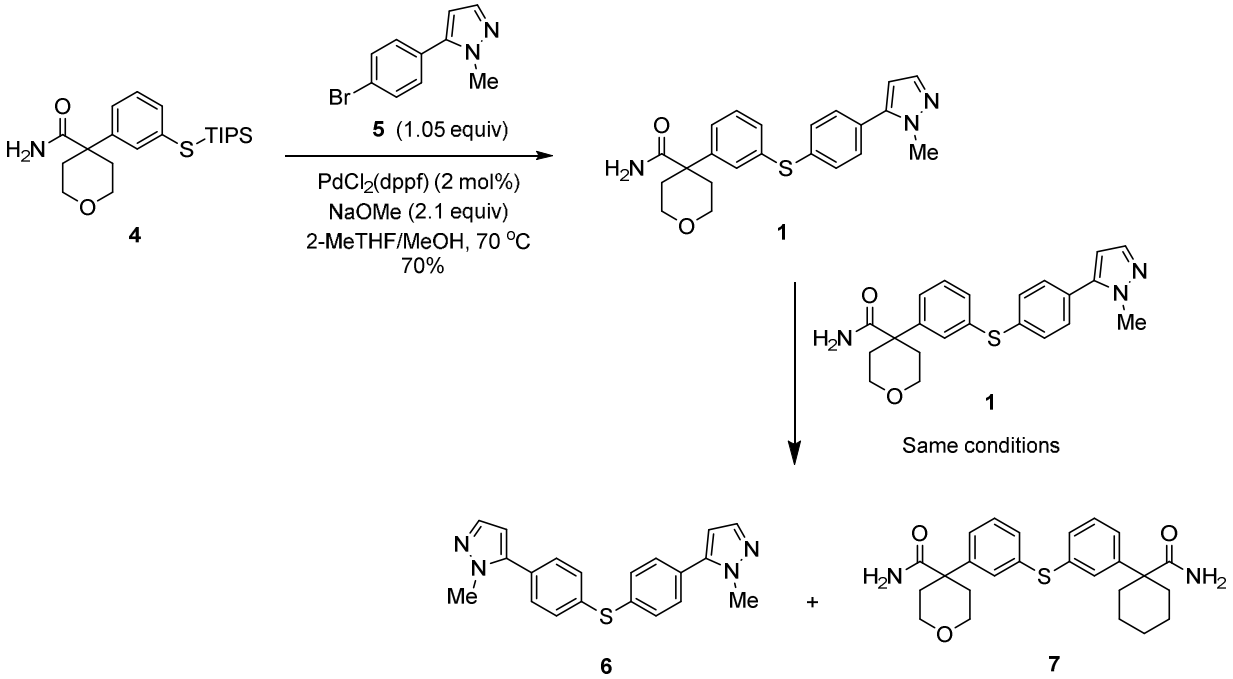

Scheme 2 Migita coupling by-products

Discussion and Results

Evaluation of the sulfur source for initial Migita coupling

In the early stages of development, we considered both bromides **2** and **5** as substrates for the initial Migita coupling. Based on factors including cost, availability, odor, and complexity of the transformation, we began exploring alternatives to TIPS-SH for the sulfuration of bromide **5** to thiophenol **8**: S_8,[6] ClSSCl,[7] CH_3COSK,[8] thiourea,[9] and NaSCN/NBS.[10] Among all the candidates, molecular sulfur (S_8) is the most desirable for its low cost, availability, and benign smell. While metalation of aryl bromide **5** with *n*-BuLi at −78 °C generated an aryllithium, alkylation of the resulting butyl bromide (byproduct of metal-halogen exchange) proceeded to **9** prior to reaction with S_8 (Scheme 3). Alternatively, the reaction of **5** with Bu_3MgLi followed by S_8 successfully provided the thiophenoxide; however, this intermediate was alkylated by butyl bromide to form **10** before it could be intercepted with an electrophile (e.g., Ac_2O, AcOH).

Employing Rieke Mg successfully generated the arylmagnesium in the absence of BuBr; however, reaction with S_8 or ClSSCl afforded a mixture of sulfide, disulfide, and trisulfide products **11**–**13**. Potassium thioacetate was reported to couple with aryl halides at 150–160 °C under microwave irradiation,[8] but we were unable to adapt this chemistry to more process-friendly conditions. Thiourea coupled successfully with **5**, but the resulting thioamidine decomposed to sulfide **11** under the reaction conditions. Furthermore, attempts to introduce sulfur onto desbromo-**5** via NaSCN/NBS[10] provided **14** via chemoselectivity for the pyrazole over the arene.

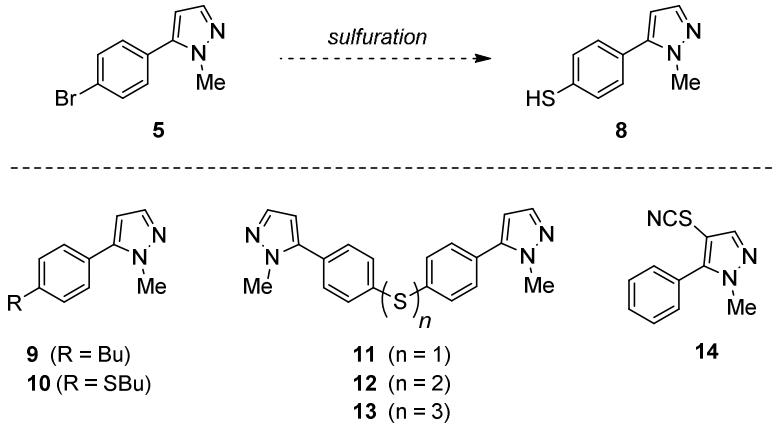

Scheme 3 Byproducts **9–14** from attempts to convert bromide **5** to thiophenol **8**

These unsuccessful attempts led us to consider several commercially-available 3-mercaptopropionates as reagents for an initial Pd-catalyzed Migita coupling (Scheme 4). Treatment of these coupling products with base would then liberate the free thiophenols (via acrylate byproducts) for a second Migita coupling. Recognizing the alkyl acrylate side products as potential Michael acceptors, a risk assessment was performed. It was concluded from the review of the scientific literature,[11] that although alkyl acrylates are clastogenic in mammalian cells *in vitro,* based on the mutagenicity and carcinogenicity profile of structurally similar acrylates, the weight-of-evidence is that *iso*-octyl acrylate and *n*-propyl acrylate, the transesterification product between the initially formed *iso*-octyl acrylate and *n*-propanol in the solvent, are not mutagenic or genotoxic carcinogens. Vogt *et. al.* reported that the primary route of detoxification involves hydrolysis by carboxylesterases found in a number of tissues, which result in the release of acrylic acid and the corresponding alcohol.[11e]

From an environmental standpoint, 3-mercaptopropionates of higher alcohols tend to be less odorous due to their large molecular weight. For instance, compared to the methyl and ethyl analogs, propyl 3-mercaptopropionate (**15**) has the advantage of a weaker odor. 2-Ethylhexyl 3-mercaptopropionate (**16**)[12], an excellent source of sulfur, has only a faint odor. Its isomer, *iso*-octyl 3-mercaptopropionate (**17**), also has little odor. From availability and cost perspectives, **17** had the advantage of bulk availability as a commodity material used in the polymer industry. Since all alkyl 3-mercaptopropionates exhibit very similar reactivities, **17** was finally chosen for development.

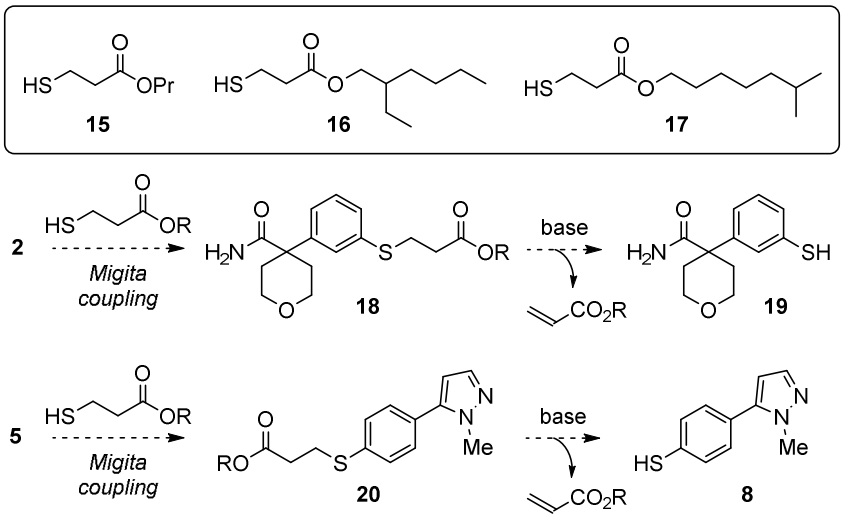

Scheme 4 3-Mercaptopropionates for the initial Migita coupling

Selection of metal catalyst and coupling partners

As per the medicinal chemistry synthesis (Scheme 1), we planned to build the thioether **1** through a sequence of two Migita couplings. It has been well documented that bidentate ligands are superior for Migita coupling and $Pd_2(dba)_3$/Xantphos is an excellent combination for this transformation.[12] Besides Pd, other base metal catalysts have been reported for Migita couplings such as Cu,[13] Ni,[14] Fe,[15] and Co;[16] however, in our hands only Pd proved efficient for both C–S bond formations en route to **1**, and so we moved forward with Pd catalysts despite their higher cost relative to other metals.

In addition to $Pd_2(dba)_3$/Xantphos, in recent years, Hartwig had demonstrated the high efficiency of $Pd_2(dba)_3$/Josiphos in Migita couplings.[5,17] Screening of palladium sources and ligands quickly identified these two as the most efficient combinations. Since Josiphos is patented and more expensive, $Pd_2(dba)_3$/Xantphos became the catalyst of choice for our process. Furthermore, $Pd_2(dba)_3$/Xantphos appeared to minimize formation of the symmetrical sulfides, which greatly reduced the burden on product purity upgrade.

We investigated the order of C–S bond formation. Since bromide **2** coupled well with 3-mercaptopropionates for the first C–S bond, we turned our attention to the second C–S bond formation (Scheme 5). The coupling of bromide **5** and thiophenol **19** performed better than the converse coupling of bromide **2** and thiophenol **8** using $Pd_2(dba)_3$ and Xantphos. Thus, we decided to first prepare thiophenol **19** via sulfuration of **2** with a 3-mercaptopropionate, and then complete the API synthesis with a second Migita coupling of **19** and bromide **5**.

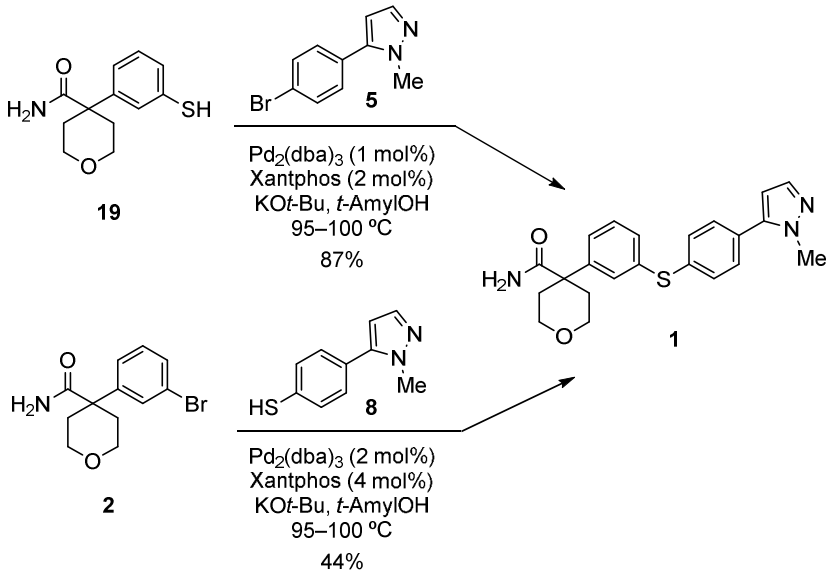

Scheme 5 Selection of the coupling partners for the second Migita coupling

Development of a one-pot, two-Migita coupling process

We set out to develop a one-pot, telescoped process[18] for the following three-step sequence: (1) Migita coupling of bromide **2** and *iso*-octyl 3-mercaptopropionate (**17**); (2) unmasking of the first Migita product **21** to thiophenol **19**; (3) second Migita coupling of **19** and bromide **5**. Two main objectives were identified to reduce the cost of the process after a preliminary analysis. Since the cost of the palladium/ligand represented the largest cost contribution, minimization of the catalyst loading was paramount. Additionally, reduction of the number of units of operation was pursued to reduce the operational cost of the process. In laboratory experiments (Scheme 6), we found that 1 mol% $Pd_2(dba)_3$ and 2 mol% Xantphos performed quite well for the first Migita coupling of bromide **2** and *iso*-octyl 3-mercaptopropionate (**17**). We were able to reduce the

Pd/Xantphos ratio from 1:2 to 1:1 without much change in performance; however, longer reaction times were necessary when lowering the catalyst loading to 0.5 mol%. Thus, we heated a mixture of bromide **2**, thiol **17**, $Pd_2(dba)_3$, Xantphos, and $(i\text{-Pr})_2NEt$ in toluene at reflux for 1 h to afford thioether **21** in >97% (HPLC).

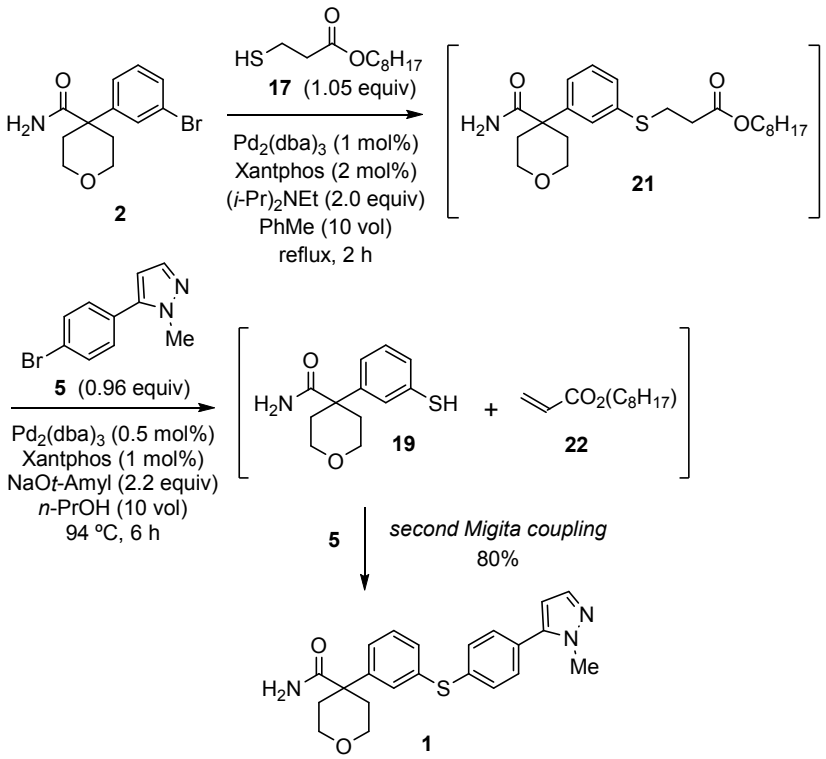

Scheme 6 Piloting a three-step, one-pot process for synthesis of **PF-04191834** (**1**)

We were gratified to discover we could telescope this reaction directly into thiophenol deprotection and subsequent Migita coupling. The mixture of **21** (while at reflux) was treated with a solution of NaO*t*-Amyl, bromide **5**, and $Pd_2(dba)_3$/Xantphos in *n*-PrOH. These basic conditions rapidly cleaved the 3-mercaptopropionate to thiophenol **19** and acrylate **22** (a strong base is required). The binary *n*-PrOH/toluene system was held at reflux for 6 h as the liberated thiophenol coupled with **5** for the second C–S bond formation. The second charge of catalyst and ligand, while not always required on laboratory scale, was added on large scale as a precaution to facilitate complete conversion to **PF-04191834** (**1**). Upon reaction completion (<3% of bromide **5** left by HPLC), the mixture was cooled to 70–80 °C and quenched with water. The phases were allowed to separate and the aqueous layer was extracted once with *i*-PrOAc. The combined

organic layers were treated with 1,2-diaminopropane (1,2-DAP)[19] and Darco G-60 (for removal of residual Pd) at 70–80 °C for 30–45 min, filtered while still heated, and concentrated for crystallization upon MeOH addition and cooling at 0 ºC. The product was isolated by filtration followed by drying under vacuum for more than 12 h. This overall process afforded the API in 80% yield over three steps on laboratory scale.

Impurity control

During the development of the chemistry for the synthesis of **PF-04191834** (**1**), a number of impurities had been observed, and their origin rationalized (see Scheme **7**). Gratifyingly, the employment of Xantphos as supporting ligand sequestered the formation of symmetrical sulfides **6** and **7**, to very low levels below 0.1%. Formation of acids **23** and **29** was managed by controlling the water content in formation of sulfide **21**, by azeotropic distillation of toluene. The formation of disulfide **24** was reduced by minimizing the exposure of the reaction mixture to air to prevent the oxidation of thiolate **26**. Impurity **28** was managed by maintaining moderate reaction temperature (the 1,4-addition pathway was found to be very temperature dependent). In addition, good purity upgrades were observed in the isolation of the crude API and ensuing polymorph control step. With these measures in place, all impurities generated in the three-step-one-pot process were driven to <0.1% level but one, which varied from 0.15–0.25%. Structure elucidation work identified the impurity as **27**. Extensive solubility-based purging studies were perform but did not afford any conditions that consistently remove this impurity.

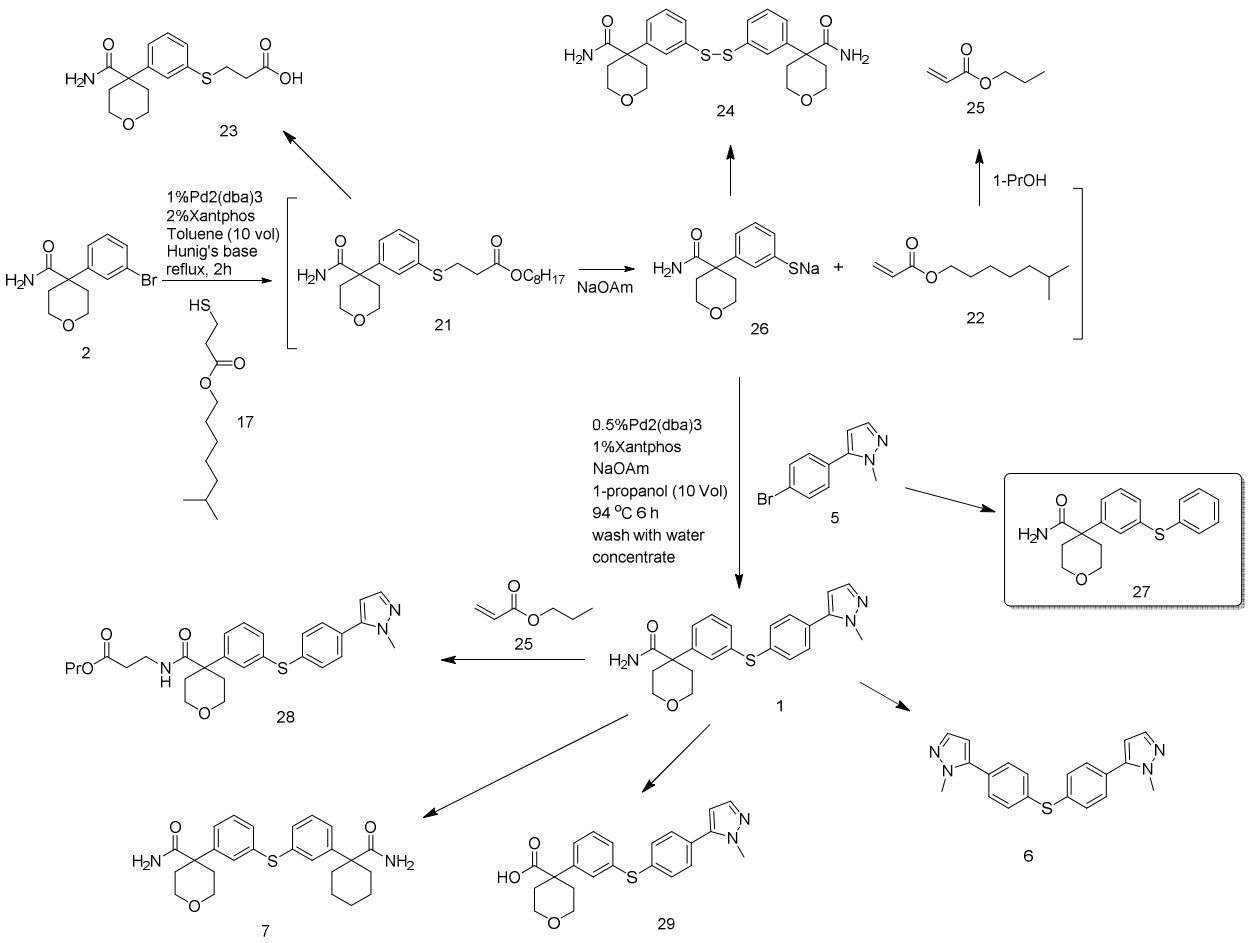

Scheme 7 Origin of impurities

Since the purge of **27** appeared difficult, its formation was studied in hope of minimizing its formation during the reaction. It was postulated that a reasonable source of this impurity is from the exchange between the palladium-bound aryl group (derived from **5**) and the phosphine-bound phenyl group,[20] a phenomenon also observed by Hartwig in his mechanistic study on C–S reductive elimination,[21] as well as researchers from Merck.[22] *A priori*, the exchange between phosphine- and palladium-bound aryl groups can occur either after oxidative addition[23] (on intermediate **II**; Figure 2) or after transmetalation (on intermediate **III**) via a C–P reductive elimination (to form a phosphonium ion)/C–P oxidative addition mechanism[24] prior to C–S reductive elimination. Although both scenarios offer a plausible pathway to the impurity, some lingering questions remained: (1) Xantphos has been employed by us and others for years in various Pd-catalyzed transformations without observations of aryl scrambling, so why does this side reaction occur in Migita coupling?[22~~22~~b] (2) Is it possible to locate the point in the catalyst

Formatte

cycle that aryl exchange occurs,[25] and hence manipulate the reaction conditions to disfavor the pathway leading to this **27**?

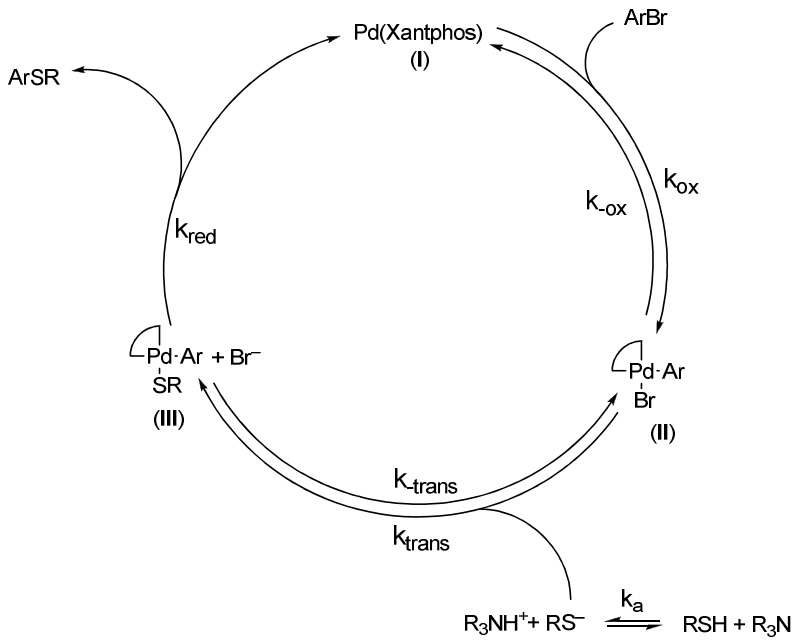

Figure 2 Catalytic cycle for Migita coupling

Kinetic Study

In order to gain insights into the Migita coupling reactions, a kinetic study was performed. Since Novak and Grushin have established that the aryl exchange occurs in the resting state of the catalyst,[23] the goal of the study was to identify the resting state of the catalyst under our conditions of Migita coupling. Based on the catalytic cycle of Migita coupling, as depicted in Figure **2**, the rate of the reaction is defined by equation (1).[26]

$$rate = k_{oxd}\frac{[Pd^*]_{total}}{1+\frac{k_{oxd}[ArBr]}{k_{red}\cdot\frac{k_{trans}\cdot\frac{K_{ab}[RSH]\cdot[DIPEA]}{[DIPEAH^+]}}{k_{red}+k_{-trans}[Br]}}+\frac{k_{trans}\cdot\frac{k_{oxd}[ArBr]}{k_{red}+k_{-trans}[Br]}\cdot\frac{K_{ab}[RSH]\cdot[DIPEA]}{[DIPEAH^+]}}{k_{red}+k_{-trans}[Br]}}\cdot[ArBr] \quad (1)$$

Note that during the deduction of the rate law RSH was not specified as alkyl- or aryl-thiol, equation (**1**) is applicable to both the first and the second Migita coupling. By inspecting equation (**1**), one very important conclusion one can draw is that the rate is first order in $[Pd]_{total}$. In order to keep the kinetic study within reasonable complexity, it is important to maintain $[Pd]_{total}$ constant as a known value. It was felt that the first step is a better candidate for this study. We reasoned that for the second Migita coupling, to keep the concentration of $[Pd]_{total}$ constant could be hard to achieve, as there are two sources of palladium/ligand in this step, i.e. the recycled catalyst from the first step and the freshly charged. Experimentally, it is very difficult to measure the concentration of the ligated palladium as against colloidal palladium. On the other hand, all reagents are used fresh in the first Migita, it is much more practical to control the concentration of the catalyst. For above considerations, the kinetic study was conducted on the first step. However, as pointed out already, the conclusion should be illustrative for both steps, considering that the catalytic cycles are the same and the differences between coupling partners are incremental.

The first goal of this study was to establish the rate law of the reaction. Reaction Progression Kinetic Analysis (RPKA) protocol employed by Blackmond[27] was selected for this study, and the *iC Kinetics* software was used to process the data. Considering the reaction was quite fast (on the time scale of minutes), the in-situ PAT monitoring approach was utilized to serve our purposes better than the off-line (HPLC) analysis, (off-line samples were indeed taken and analyzed to confirm the reaction completion).

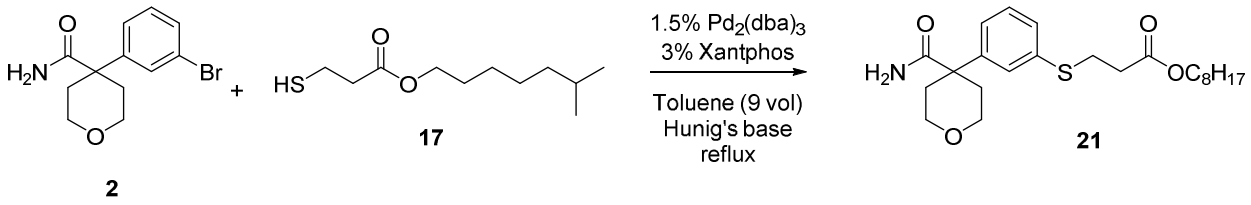

2 **17** **21**

Scheme 8 Formation of thioether **21**.

The formation of thioether **21** was hence carried out with simultaneous in-situ IR/Raman monitoring. Gratifyingly, the disappearance of **2** (ArBr) and *iso*-octyl-3-mercaptopropionate (**17**, RSH) could be monitored by Raman and the formation of **21** could be monitored by IR

simultaneously in real time, a typical graph of concentration change against time is shown in Figure **3**.

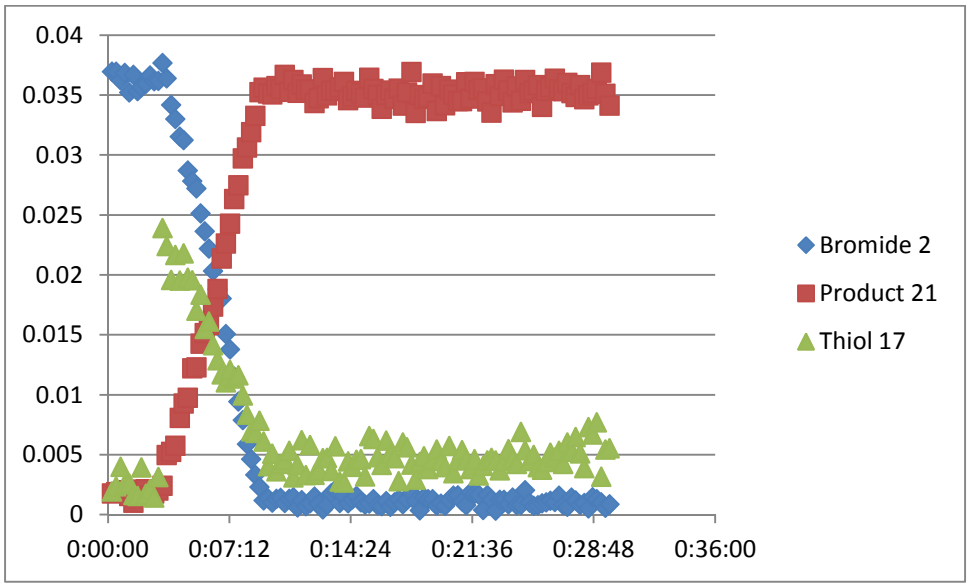

Reaction conditions: a mixture of bromide **2** (4.00 g, 14.1 mmol), $Pd_2(dba)_3$ (194 mg, 0.212 mmol, 1.5 mol%), Xantphos (244 mg, 0.422 mmol, 3.0 mol%), Hunig's base (4.92 mL, 28.3 mmol, 2.0 eq.) in 36.0 mL of toluene was degassed and heated to a vigorous reflux, *iso*-octyl-3-mercaptopropionate (3.60 mL, 16.1 mmol, 1.14 eq.) was added bolus through a septum. The progression of the reaction was monitored simultaneously by both an IR probe and a Raman probe: Raman trend of bromide **2** (blue) and *iso*-octyl-3-mercaptopropionate (green); IR trend of thioether **21** (red). The disappearance of the bromide, the thiol, as well as the formation of the thioether all exhibited linear behavior against time. (Note: in the developed process, lower catalyst loading was employed, as it was found that such high catalyst loading was unnecessary.)

Figure 3. Real time monitoring for the formation of thioether **21**.

From the same excess experiments, the overlay (see Figure **4**) of the two curves indicated that at this time scale, no extensive catalyst deactivation or product inhibition occurred, and deemed this transformation "well-behaved".

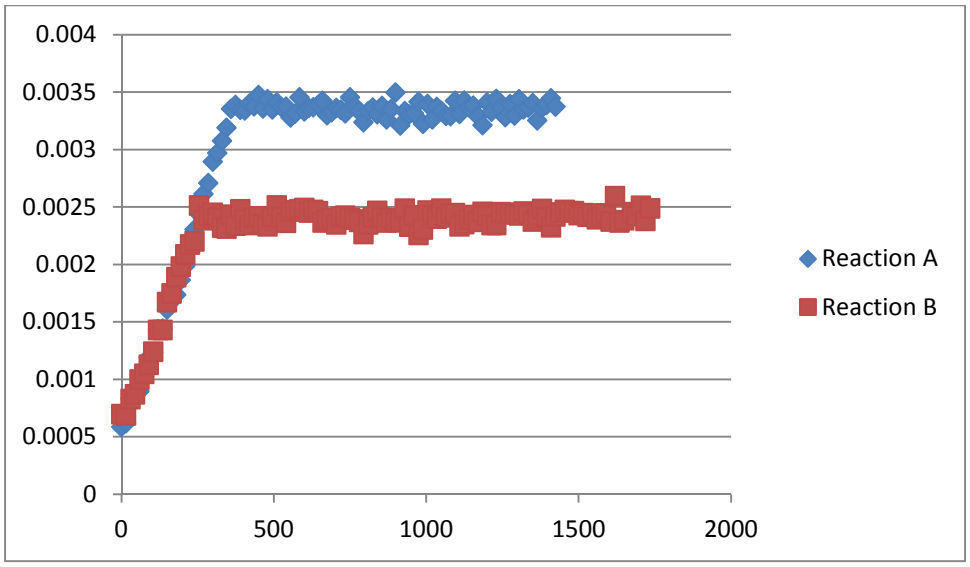

Initial concentration of Reaction A: $[Pd]_0$= 0.0086 M, $[ArBr]_0$= 0.288 M, $[RSH]_0$= 0.329 M,[Excess]= 0.041 M; Initial concentration of Reaction B: $[Pd]_0$= 0.0086 M, $[ArBr]_0$= 0.202 M, $[RSH]_0$= 0.243 M,[Excess]= 0.041 M; Reaction condition: a mixture of bromide **2**, $Pd_2(dba)_3$, Xantphos, Hunig's base in toluene was degassed and heated to a vigorous reflux, *iso*-octyl-3-mercaptopropionate was added bolus through a septum. The formation of thioether **21** was monitored by IR probe.

Figure **4** Same excess experiment for the formation of thioether **21**

Performing the same reaction at different initial concentrations of **2** (ArBr) but same *iso*-octyl-3-mercaptopropionate (**17**, RSH) concentration (different excess), the kinetic behavior of the reactants was analyzed with *iC Kinetics* software and the power law was deduced as **Rate=0.00083[RSH]$^{0.00}$[ArBr]$^{0.13}$ (T=110 °C)**, see Figure 5. Within the sensitivity of IR and Raman, no sign of change of mechanism from low conversion to high conversion was observed.

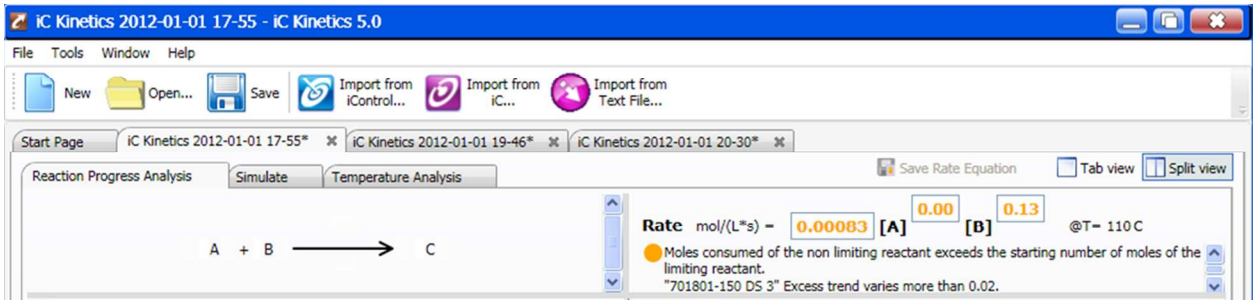

Initial concentration of Reaction A: $[Pd]_0$= 0.0086 M, $[ArBr]_0$= 0.288 M, $[RSH]_0$= 0.329 M,[Excess]= 0.041 M; Initial concentration of Reaction B: $[Pd]_0$= 0.0086 M, $[ArBr]_0$= 0.202 M, $[RSH]_0$= 0.329 M,[Excess]= 0.127 M; Reaction condition: a mixture of bromide **2**, $Pd_2(dba)_3$, Xantphos, Hunig's base in toluene was degassed and heated to a vigorous reflux, *iso*-octyl-3-mercaptopropionate was added bolus through a septum. The formation of thioether **21** was monitored by IR.

Figure 5. Different excess experiment for the formation of thioether **21**

Based on the observation that the concentration vs. time plot is linear (within experimental error, *vide supra*) and the output of *iC Kinetics*, it appeared that the Migita coupling is zeroth order in both **2** (ArBr) and *iso*-octyl-3-mercaptopropionate (**17**, RSH). As depicted in the mechanism of the Migita coupling summarized in Figure **2**, the catalytic cycle is composed of three steps: oxidative addition, transmetallation, and reductive elimination. Since the rate law indicated that the reaction is zeroth order in both the aryl bromide and the thiol, it meant that those two components are not involved in the rate limiting step, which suggested that the reductive elimination step is the rate limiting step, a kinetic model that closely resembled palladium-catalyzed C(sp)-C(sp) cross-coupling.[28] And this implied that the resting state of the catalyst is intermediate **III** in Figure **2**, where both the aryl group and the thiol are bound to the palladium center.[29]

This observation offered a good explanation for the generation of byproduct **27**. With intermediate **III** as the resting state of the catalyst, slow[30] C–S reductive elimination presented an opportunity for competitive ligand dissociation/C–P reductive elimination from **31**[23b] and subsequent oxidative addition to the Ph–P bond en route to **27** (see Scheme 9). It should be pointed out that for most of the Pd(Xantphos)-mediated transformations, oxidative addition is the rate limiting step.[4] This suggests that typically Pd(Xantphos) **I** is the resting state of the catalyst rather than intermediate **III** type, which is perhaps the reason for the scarce citation of this side reaction.

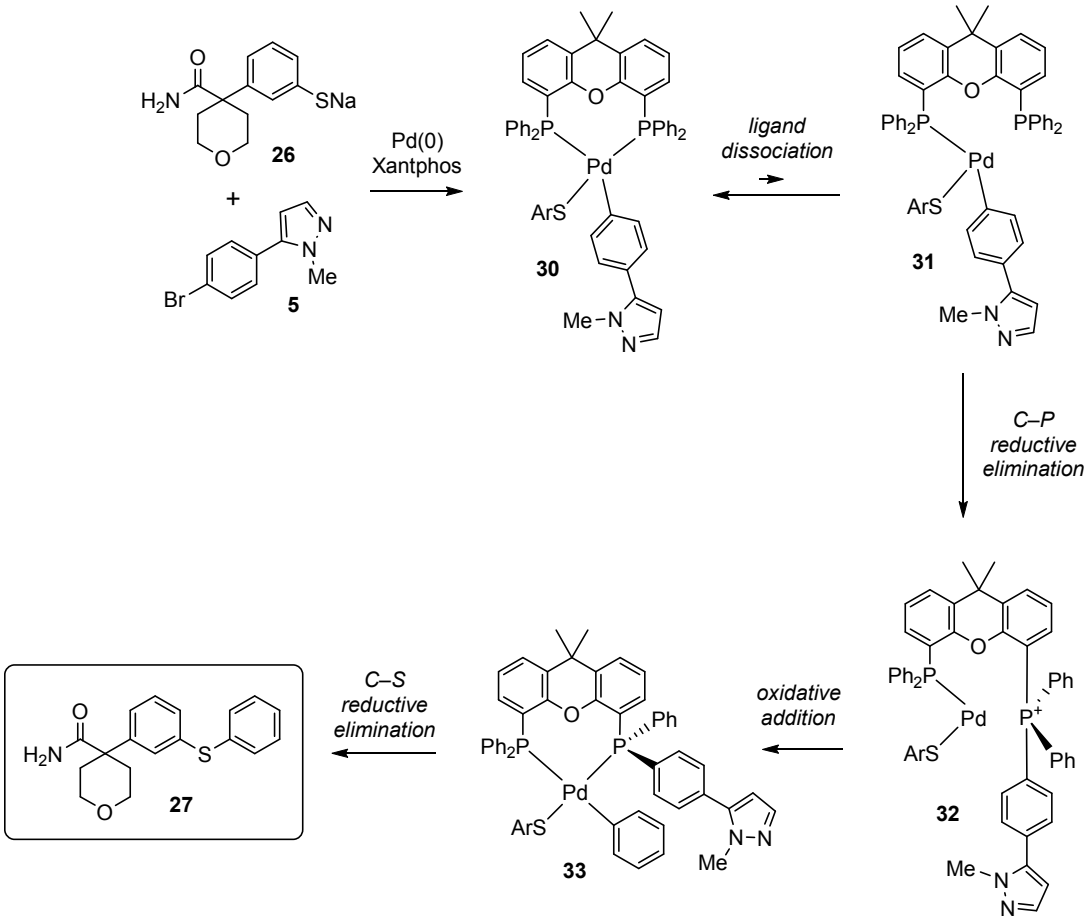

Scheme 9 Proposed pathway to impurity **27**

This kinetic analysis also offered a rationale for the empirically discovered conditions that minimized the formation of **27** (i.e. performing the reaction at lower temperature and reducing the *n*-PrOH to toluene ratio). Presumably, at lower temperature, dissociation of one phosphine

from **30** became much more difficult, hence suppressing C-P reductive elimination; also, reduced *n*-PrOH to toluene ratio lowered the polarity of the reaction medium, which further hampered C–P reductive elimination/oxidative addition pathway, consistent with Novak's observation of the effect of lower solvent polarity on aryl exchange.[23~~23~~a] Under the modified conditions, the second Migita coupling became substantially slower and required >10 h to reach completion (still an acceptable reaction time to be practical); however, under such conditions, **27** did not form in any appreciable amount (*vide supra*).

Formatte

Crystallization of PF-04191834 (1) with color removal and polymorph control

Several polymorphs have been identified for PF-04191834 (**1**), and we need to develop a workup and crystallization to ensure isolation of API with the desired form (designated Form A) and purity. Solid form studies had identified three anhydrous polymorphs: Forms A, B, and C. In addition, solvated forms with acetone and CH_2Cl_2 were discovered during early polymorph screening studies. Competitive slurry studies demonstrated that Form A was the most stable of these three anhydrous forms at room temperature. Additional solid form characterization studies determined that Forms A and B are enantiotropically-related polymorphs, with Form B being the more stable above a transition temperature determined to be in the range of 63–100 °C. When the API is already present in high purity, it crystallizes out of THF as Form A; however, this process offered very limited purity upgrade when less pure material was employed. With this understanding of the polymorph landscape for **1**, a recrystallization process was developed to purge impurities and ensure isolation of the desired form.

As shown in Scheme 6, we prepared **1** in a binary solvent system of *n*-PrOH and toluene, and we explored mixtures of these two solvents for API recrystallization. Kinetic solubility and metastable zone limit (MSZL) data of the API in 23.7% *n*-PrOH/toluene (a specific binary system that was found empirically to have the highest dissolving power for the API at 90 °C) was measured as a function of temperature. These data illustrate that **1** has a rather wide metastable zone width of approximately 30 °C (Figure 6, cooling rate=0.2 °C/min.). Based on this measured solubility data, a process was developed in which the crude API was dissolved in approximately 35 mL/g of the *n*-PrOH/toluene

combination at 80 °C. The resulting mixture was a deep red color, and close inspection showed the batch contained a thin haze of colored particulate. This non-dissolved material (origin of dark color) was subsequently removed by filtering the batch through Celite, which had been preheated to prevent the sudden crystallization of API during the transfer. Inspection of the Celite bed after the filtration showed a covering of dark orange material on the surface with substantially less color deeper into the bed.

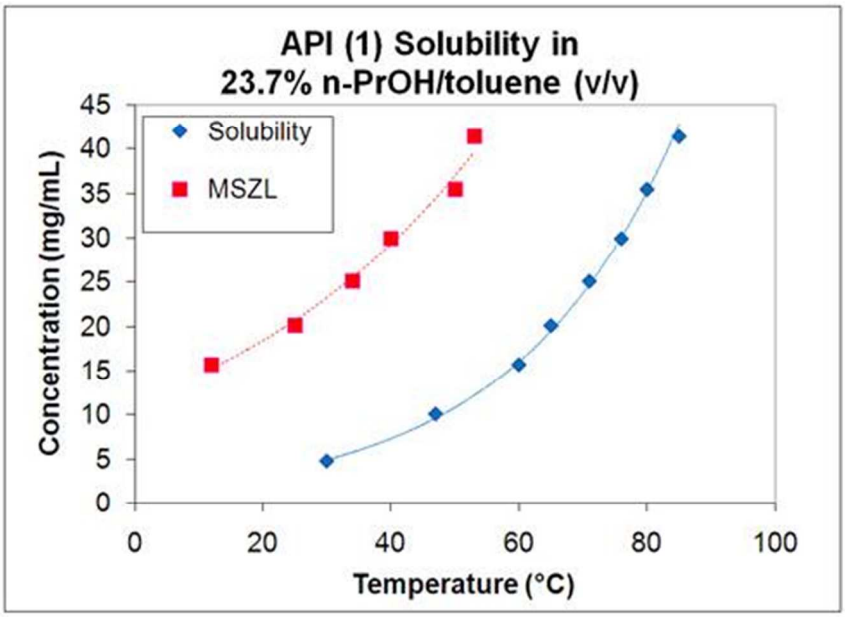

Figure 6 Kinetic solubility and metastable zone limit data for **1** in 23.7% *n*-PrOH/toluene mixture as a function of temperature

The resulting pale yellow filtered solution was cooled below 40 °C to induce supersaturation, and seeded with 0.2 wt% of Form A crystals to induce nucleation of the desired form. It was observed that the system may be slow to crystallize at 40 °C, and reducing the temperature to 20 °C promoted the crystallization of the API. Partial vacuum distillation of solvent further promoted crystallization of **1** from the mother liquor. At this point in the process, the resulting slurry typically contained a mixture of the metastable Form B along with the desired Form A. Extended stirring between 20–45 °C allowed for polymorph conversion to the desired Form A. The upper-end of the temperature range for the polymorph conversion remained below the

transition temperature between Form A and Form B, which may be as low as 63 °C. Testing by powder x-ray diffraction (PXRD) of an in-process sample was used to determine that complete conversion to the desired form had been achieved. Once the PXRD analysis was complete, the batch was held between 0–5 °C to maximize yield. After filtration, the batch was washed by toluene followed by *n*-PrOH.

Final commercial process on multikilogram scale

With the developmental issues resolved, the process was demonstrated on multikilogram scale (Scheme 10). The three-step, one-pot process successfully converted 28.0 kg of bromide **2** and 21.0 kg of bromide **5** to 25.0 kg (72% yield) of the crude API as a MeOH-wet cake with 99.1% purity. (A decision was made not to perform the carbon treatment during the workup.) Assay of the mother liquor suggested the loss of ~10% API which was not pursued. Next, the polymorph control step was executed to demonstrate control of impurities. Thus, the crude API was charged to the reactor as a MeOH-wet cake from the previous step. This residual MeOH had no impact on the recrystallization process as it was removed by atmospheric distillation prior to *n*-PrOH addition. Due to the challenge of confirming API dissolution because of insoluble colored particulate and limited sight in the pilot-plant reactor, an additional 7 volumes of toluene were added to the batch to ensure dissolution. Special care was taken to ensure that the Nutsche filter containing the Celite bed and the subsequent cartridge filter remained at 75 °C to prevent the crystallization of the API during the filtration step. The batch was concentrated via partial vacuum distillation and cooled to <20 °C to promote API crystallization. PXRD analysis of an in-process sample after 10 h of stirring at 45 °C indicated the presence of Form A alone. With the desired polymorph confirmed, the batch was cooled to <5 °C, filtered and washed with toluene followed by *n*-PrOH.

After the purity upgrade and polymorph control step, 19.9 kg of **PF-04191834** (**1**) as Form A was isolated with 99.6% HPLC purity but contained 300 ppm residual Pd without additional treatment to purge palladium (Scheme 10). The carbon treatment was executed to purge residual palladium (Thiol-3 functionalized silica was equally effective; carbon was selected for lower cost). Accordingly, the API was dissolved in 45 volumes of THF at 45 °C and treated with

20 wt% of activated carbon for 18 h. The mixture was filtered, concentrated, and charged with heptane as antisolvent to precipitate the API in high recovery. After filtration and drying, 19.3 kg of API was isolated in 97% yield with 99.7% purity (HPLC) and <1 ppm Pd. The overall yield of the entire process was 55%.

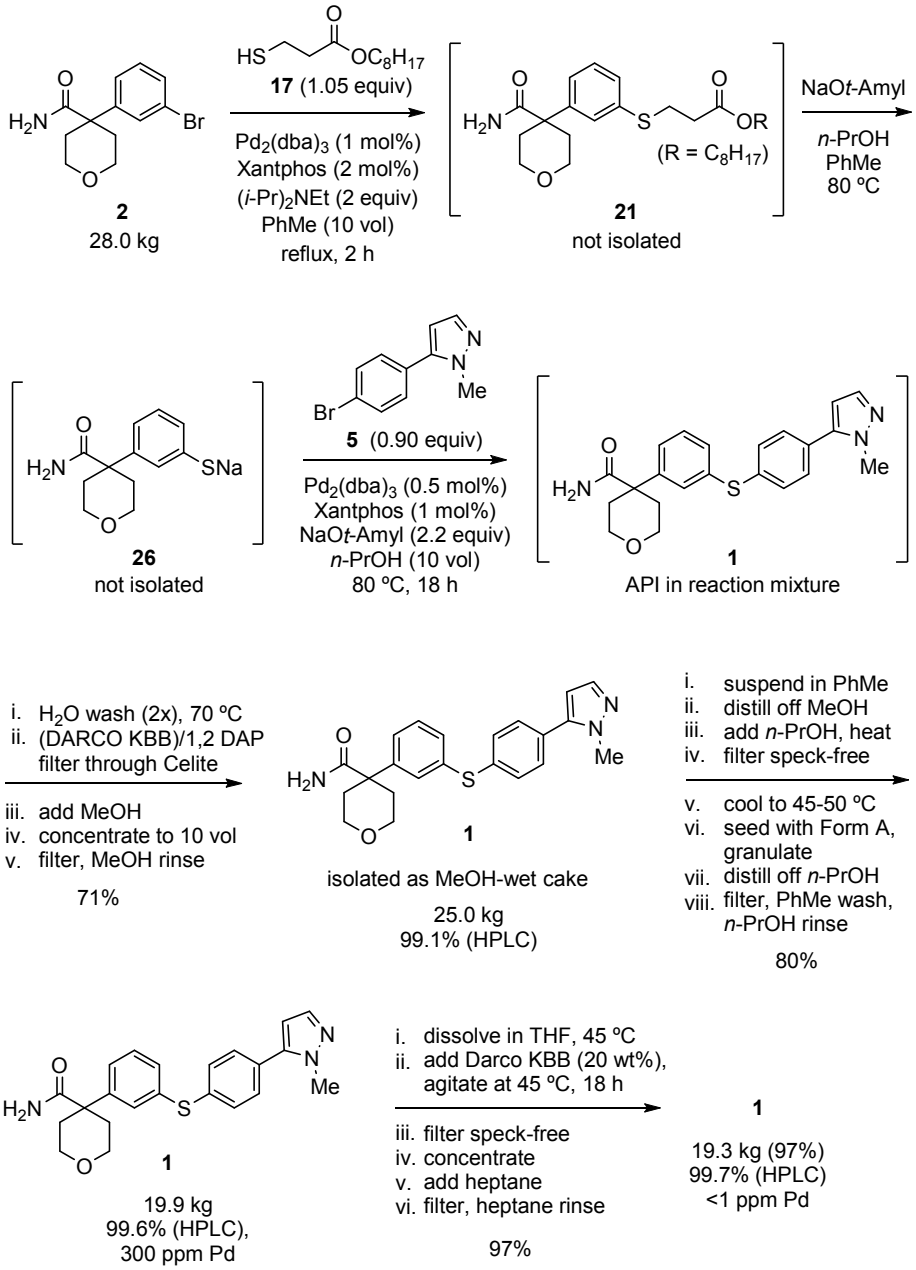

Scheme 10 Multikilogram-scale production of **PF-04191834** (**1**)

Conclusion

We developed a three-step, one-pot process for the synthesis of **PF-04191834** (**1**) via a sequence of two Migita couplings. This strategy employed cheap, odorless, and readily-available *iso*-octyl 3-mercaptopropionate as the sulfur source for the initial Migita coupling as a general alternative to the popular TIPS-SH for the formation of diaryl thioethers. A kinetic study revealed that at high temperature, reductive elimination could be the rate limiting step in the catalytic cycle, which opens pathways for the generation of undesired impurities. By properly controlling the reaction conditions, the desired API was synthesized in 72% crude yield and 55% isolated yield after purification. This process was successfully demonstrated on 20-kg scale.

Experimental

General Procedures Intermediates were analyzed by reverse phase LC–MS on an Agilent 1100 series instrument, coupled to a Waters Micromass ZQ mass spectrometer according to the following conditions: column Extend-C18 3.0 mm × 50 mm i.d., 1.8 μm; eluent A, 5% v/v acetonitrile in 10 mM aqueous ammonium acetate; eluent B, acetonitrile; flow rate 1.2 mL/min; wavelength, diode array (190–400 μm); column temperature, 50 °C; injection volume, 10 μL; at t = 0 min, 5% eluent B; at t = 3.5 min, 100% eluent B; at t = 4.5 min, 100% eluent B; at t = 4.6 min, 5% eluent B. ^{1}H and ^{13}C NMR spectra were recorded on a Bruker Ultrashield 400 Plus spectrometer at 400 and 100.6 MHz, respectively. The quoted melting points for all materials are the onset temperatures observed by DSC.

Formation of the crude API (1): A 300 gal reactor was charged with 28.0 kg (98.6 mol) of bromide **2** and 292 kg (336 L) of toluene. Under nitrogen protection at atmospheric pressure, ~10 gal of toluene was distilled out to remove stray and surface water. After the contents had been cooled to 30 °C, the reactor was charged with 0.90 kg of $Pd_2(dba)_3$, 1.14 kg of Xantphos, 25.47 kg of diisopropylethylamine, and 22.6 kg of iso-octyl-3-mercaptopropionate (**17**). The vessel was thoroughly degassed by alternately connecting the head space to house vacuum and ultra pure nitrogen. The contents in the vessel were heated at reflux for 90 min, at which time, an off-line sample indicated all bromide **2** was consumed and the desired thioether **21** had formed. While maintaining the internal temperature at 80 °C, the vessel was charged with 134.4 kg (168 L) of 1-propanol, a warm (50 °C) solution of 25.7 kg of NaO-*t*-Am in 134 kg (154 L) of toluene,

followed by a 26 kg (33 L) 1-propanol chase. The contents were then allowed to heat at 80 °C for 1 h. The vessel contained thiolate **26** at this point.

While maintaining the internal temperature at 80 °C, the vessel was charged a solution of 21.03 kg of aryl bromide **5** in 36.6 kg (42 L) of toluene, followed by a mixture of 0.57 kg of Xantphos and 0.45 kg of $Pd_2(dba)_3$ in 14.1 kg (16.6 L) of toluene. The contents in the tank were allowed to heat at 80 °C for 18 h, at which time, off-line HPLC assay indicated the consumption of aryl bromide **5** and the formation of the desired API.

Isolation of the crude API. The temperature of the contents was brought to 70 °C and 84 kg of water was added. After agitation for 30 min at 70 °C, the phases were allowed to split and the lower aqueous layer was removed. The organic phase was washed one more time with 84 kg of water at 70 °C. To the organic phase was charged 27.76 kg of 1,2-diaminopropane,[31] and the contents in the vessel was heated for one hour at 70 °C, filtered through a pad of Celite in a pre-heated Nutsche filter, and concentrated from a total volume of ~250 gal to ~105 gal at 35 °C under vacuum. To the mixture was charged 66.3 kg (84 L) of methanol, and the mixture was allowed to heat at 55 °C for 30 min. After cooling to 5 °C and granulating for 12 h, the mixture was filtered, and the cake was washed with 66.4 kg (84 L) of cold methanol. After pulling dry, the methanol-wet cake weighed 43.7 kg.

Karl-Fischer assay and GC head space analysis indicated that the material contained 1.36% water and 41.3% methanol, which translate to 25.0 kg (72% over three steps) of the crude API on dry basis. Evaluation of the mother liquor indicated that ~10% of the API was lost to the mother liquor, no efforts were made to recover this material.

Purity upgrade. The wet cake was charge to a 300 gal vessel, followed by 337.5 kg (389 L) of toluene. Methanol was distilled out under atmospheric pressure until the pot temperature reached 80 °C. To the vessel was charged 150 kg of 1-propanol, and the resulting mixture was heated at 80 °C for 2 h, until a clear solution formed. The temperature of the solution was brought to 45 °C, seeded with form B crystals, and aged for 18 h, at which time, a thick slurry formed. The slurry was chilled to 5 °C, aged for 2 h, filtered, washed with 32.62 kg of toluene to afford 19.9 kg of pure API after drying under vacuum. Mp 173 °C. ^{1}H NMR (400 MHz, DMSO-d6) 7.52

(2H, m), 7.48 (2H, m), 7.42 (2H, m), 7.35 (2H, m), 7.29 (2H, m), 7.07 (1H, br. s), 6.42 (1H, d, J = 1.8 Hz), 3.85 (3H, s), 3.74 (2H, dt, J = 11.7, 3.7 Hz), 3.47 (2H, br. t, J = 11.7 Hz), 2.41 (2H, br. d, J = 13.3 Hz), 1.80 (2H, m). ^{13}C NMR (100.6 MHz, DMSO-d6) 174.6, 146.0, 141.9, 137.9, 136.0, 133.2, 130.1, 129.7, 129.4, 129.3, 128.6, 125.6, 105.9, 64.6, 47.8, 37.6, 33.9. LCMS: found m/z 394.17 [M + H]+. Anal. Calcd for $C_{22}H_{23}N_3O_2S$: C, 67.15; H, 5.89; N, 10.68; S, 8.15. Found: C, 67.09; H, 5.93; N, 10.69; S, 8.16.

Pd removal. A glass-lined vessel was charged with 796 kg of THF, followed by 19.9 kg of **PF-04191834** (**1**). The contents were heated to 45 °C, at which time, a clear solution formed. To the solution was charged 3.98 kg of DARCO KBB and the resulting mixture was agitated at 45 °C for 14 h. The activated carbon was filtered-off and the THF solution was further filtered speck-free. The total volume of the solution was reduced to 50 gal under reduced pressure at 45 °C, yielding a suspension of the API in Form A. After cooling to 20 °C, 140.5 kg of heptane was added as anti-solvent, and the resulting suspension was allowed to agitate for an additional 30 min. The mixture was filtered and the cake was washed with 33 kg of heptane. Upon drying under vacuum, 19.3 kg of the API was isolated, which met all the pre-set specifications and was released for clinical uses. Mp 173 °C. ^{1}H NMR (400 MHz, DMSO-d6) 7.52 (2H, m), 7.48 (2H, m), 7.42 (2H, m), 7.35 (2H, m), 7.29 (2H, m), 7.07 (1H, br. s), 6.42 (1H, d, J = 1.8 Hz), 3.85 (3H, s), 3.74 (2H, dt, J = 11.7, 3.7 Hz), 3.47 (2H, br. t, J = 11.7 Hz), 2.41 (2H, br. d, J = 13.3 Hz), 1.80 (2H, m). ^{13}C NMR (100.6 MHz, DMSO-d6) 174.6, 146.0, 141.9, 137.9, 136.0, 133.2, 130.1, 129.7, 129.4, 129.3, 128.6, 125.6, 105.9, 64.6, 47.8, 37.6, 33.9. LCMS: found m/z 394.17 [M + H]+. Anal. Calcd for $C_{22}H_{23}N_3O_2S$: C, 67.15; H, 5.89; N, 10.68; S, 8.15. Found: C, 67.09; H, 5.93; N, 10.69; S, 8.16.

Acknowledgments

The authors would like to thank Drs. Stephane Caron, Juan Colberg, Joel Hawkins, Robert Singer, Sebastien Monfette, John Ragan, Nathan Ide, Zhihui Peng, Jason Mustakis, Jade Nelson, Joshua Dunetz, Michelle Kenyon, Trish Ellis as well as Javier Magano and Professors Steven Ley, David Collum, Justin Du Bois, and Donald Watson for helpful discussion. Special thanks to Drs. Stephane Caron, Robert Singer and Sebastien Monfette for proof reading the manuscript.

We thank Weiling Cai for performing important experiments in this work. We are grateful to Dr. Dominique Hebrault from Mettler for providing the initial trial version of *the iC Kinetics* software.

References

[1] Alvira, E.; Graneto, M. J.; Grapperhaus, M. L.; Iyanar, K.; Maddux, T. M.; Mahoney, M. W.; Massa, M. A.; Sample, R. K.; Schmidt, M. A.; Seidel, R. E.; Selbo, J. G.; Tollefson, M. B.; Vonder Embse, R. A.; Wagner, G. M.; Woodard, S. S. WO 2009069044 A1, 2009.

[2] Graneto, M. J.; Maddux, T. M.; Masferrer, J. L. US 20080125474 A1, 2008.

[3] (a) de Koning, P. D.; Murtagh, L.; Lawson, J. P.; Vonder Embse, R. A.; Kunda, S. A.; Kong, W. *Org. Process Res. Dev.* **2011**, *15*, 1046. Also see: (b) Mano, T.; Stevens, R. W.; Ando, K.; Kawai, M.; Kawamura, K.; Nakao, K.; Okumura, Y.; Okumura, T.; Sakakibara, M.; Miyamoto, K.; Tamura, T. *Chem. Pharm. Bull.* **2005**, *53*, 965. (c) Mano, T.; Stevens, R. W.; Okumura, Y.; Kawai, M.; Okumura, T.; Sakakibara, M. *Bioorg. Med. Chem. Lett.* **2005**, *15*, 2611. Note: In the second Migita coupling, NaOMe was employed instead of NaO-*t*-Bu, as NaOMe was found experimentally to remove the TIPS group more efficiently, see ref. 3(a).

[4] For a recent review on Migita coupling see, Beletskaya, I. P.; Ananikov, V. P. *Chem. Rev.* **2011**, *111*, 1596.

[5] Fernández–Rodríguez, M. A.; Shen, Q.; Hartwig, J. F. *J. Am. Chem. Soc.* **2006**, *128*, 2180.

[6] Brown, A. D.; Davis, R. D.; Fitzgerald, R. N.; Glover, B. N.; Harvey, K. A.; Jones, L. A.; Liu, B.; Patterson, D. E.; Sharp, M. J. *Org. Process Res. Dev.* **2009**, *13*, 297.

[7] Korn, T. J.; Knochel, P. *Synlett* **2005**, 1185.

[8] Lai, C.; Backes, B. J. *Tetrahedron Lett.* **2007**, *48*, 3033.

[9] (a) Takagi, K. *Chem. Lett.* **1985**, 1307. (b) Takagi, K. *Chem. Lett.* **1986**, 1379.

[10] Moseley, J. D.; Brown, D.; Firkin, C. R.; Jenkin, S. L.; Patel, B.; Snape, E. W. *Org. Process Res. Dev.* **2008**, *12*, 1044. Note: the role of NBS here is to convert NaSCN into a electrophile.

[11] (a) Dobo, K.; Greene, N.; Cyr, M.; Caron, S.; Ku, W. *Regul. Toxicol. Pharmacol.* **2006,** *44*; 282; (b) Seifried, H.; Seifried, R.; Clarke, J.; Junghans, T.; San, R. *Chem. Res. Toxicol.* **2006**, *19*; 627; (c) Andrews, L. S.; Clary, J. J. *J. Toxicol. Environ. Health* **1986** 19, 149; (d) Gordon, S. C., Zimmerman, D. D., Griffith, F. D. *J. Toxicol. Environ. Health* **1991**, *34*. 297; (e) Johannsen, F. R.; Vogt, B.; Waite, M.; Deskin, R. *Regul. Toxicol. Pharmacol*. **2008** *50*, 322.

[12] (a) Itoh, T.; Mase, T. *Org. Lett.* **2004**, *6*, 4587. (b) Itoh, T.; Mase, T. *J. Org. Chem.* **2006**, *71*, 2203.

[13] Huang, Y.-B.; Yang, C.-T.; Yi, J.; Deng, X.-J.; Fu, Y.; Liu, L. *J. Org. Chem.* **2011**, *76*, 800.

[14] Zhang, J.; Medley, C. M.; Krause, J. A.; Guan, H. *Organometallics* **2010**, *29*, 6393.

[15] Correa, A.; Carril, M.; Bolm, C. *Angew. Chem., Int. Ed.* **2008**, *47*, 2880.

[16] Wong, Y.-C.; Jayanth, T. T.; Cheng, C.-H. *Org. Lett.* **2006**, *8*, 5613.

[17] Hartwig, J. F. *Acc. Chem. Res.* **2008**, *41*, 1534.

[18] While our work was on-going, a TIPS-SH based one-pot protocol was published by Hartwig: Fernández–Rodríguez, M. A.; Hartwig, J. F. *Chem. Eur. J.* **2010**, *16*, 2355.

[19] Flahive, E. J.; Ewanicki, B. L.; Sach, N. W.; O'Neill–Slawecki, S. A.; Stankovic, N. S.; Yu, S.; Guinness, S. M.; Dunn, J. *Org. Process Res. Dev*. **2008**, *12*, 637.

[20] For reports on exchange of the phosphine- and palladium-bound aryl groups, see: (a) Kong, K. C.; Cheng, C. H. *J. Am. Chem. Soc.* **1991**, *113*, 6313. (b) Morita, D. K.; Stille, J. K.; Norton, J. R. *J. Am. Chem. Soc.* **1995**, *117*, 8576.

[21] Barañano, D.; Hartwig, J. F. *J. Am. Chem. Soc.* **1995**, *117*, 2937.

[22] (a) Zheng, N.; McWilliams, J. C.; Fleitz, F. J; Armstrong, J. D., III; Volante, R. P. *J. Org. Chem.* **1998**, *63,* 9606. (b) Wager, K. M.; Daniels, M. H. *Org. Lett.* **2011**, *13*, 4052.

[23] (a) Goodson, F. E.; Wallow, T. I.; Novak, B. M. *J. Am. Chem. Soc*. **1997**, *119*, 12441. (b) Grushin, V. V. *Organometallics* **2000**, *19,* 1888; [Note: Grushin established that C-P reductive elimination occurred by dissociation of one phosphine ligand first to give a coordinately unsaturated tricoordinated Pd(II) intermediate, which is competent to reductively eliminate phosphonium ion; the presence of added phosphine ligand retarded the formation of tricoordinated Pd(II) intermediate, hence disfavored C-P reductive elimination; the same observation was also made by Hartwig, see Ref. 20.]

[24] (a) Segelstein, B. E.; Butler, T. W.; Chenard, B. L. *J. Org. Chem.* **1995**, *60*, 12. (b) Kwong, F. Y.; Lai, C. W.; Yu, M.; Chan, K. S. *Tetrahedron* **2004**, *60*, 5635. (c) Marcoux, D.; Charette, A. B. *J. Org. Chem.* **2008**, *73*, 590. (d) Wakioka, M.; Nakajima, Y.; Ozawa, F. *Organometallics* **2009**, *28,* 2527.

[25] In Suzuki coupling, Novak suggests that exchange between phosphine- and palladium-bound aryl moieties occurs after oxidative addition before transmetalation (ref. 23). In ref. 22b, the authors postulate that the exchange could occur either before or after transmetalation.

[26] Based on the catalytic cycle of Migita coupling, as depicted in Figure **2**, the rate of the reaction is defined by:

$$rate = \frac{d[III^*]}{dt} = k_{red}[III\ *] \tag{2}$$

According to Briggs-Haldane approximation:

$$k_{red}[III\ *] + k\_trans[III\ *] \cdot [Br] = k_{trans}[RS^-] \cdot [II\ *] \tag{3}$$

And:

$$k_{red}[III\ *] = k_{oxd}[I\ *][ArBr] \tag{4}$$

Where:

$$[RS^-] = \frac{K_{ab}[RSH]\cdot[DIPEA]}{[DIPEAH^+]} \tag{5}$$

Substitute equation (4) into (2) and solve for [*III**]:

$$[III\ ^*] = \frac{k_{trans}\cdot[II^*]\cdot\frac{K_{ab}[RSH]\cdot[DIPEA]}{[DIPEAH^+]}}{k_{red}+k\_trans[Br]} \tag{6}$$

Substitute equations (4) and (5) into (3):

$$k_{red}\cdot\frac{k_{trans}\cdot[II^*]\cdot\frac{K_{ab}[RSH]\cdot[DIPEA]}{[DIPEAH^+]}}{k_{red}+k\_trans[Br]} = k_{oxd}[I\ *][ArBr] \tag{7}$$

Rearrange and solve for [II]:

$$[II\ *] = \frac{k_{oxd}[I^*][ArBr]}{k_{red}\cdot\frac{k_{trans}\cdot\frac{K_{ab}[RSH]\cdot[DIPEA]}{[DIPEAH^+]}}{k_{red}+k\_trans[Br]}} \tag{8}$$

Substitute (7) into (5):

$$[III\ ^*] = \frac{k_{trans}\cdot\frac{k_{oxd}[I^*][ArBr]}{k_{trans}\cdot\frac{K_{ab}[RSH]\cdot[DIPEA]}{[DIPEAH^+]}}\cdot\frac{K_{ab}[RSH]\cdot[DIPEA]}{[DIPEAH^+]}}{k_{red}+k\_trans[Br]} \tag{9}$$

Based on material balance:

$$[Pd\ *]_{total} = [I\ *] + [II\ *] + [III\ *] \tag{10}$$

$$[Pd\,*]total = [I\,*] + \frac{k_{oxd}[I^*][ArBr]}{k_{red}\cdot\frac{k_{trans}\cdot\frac{K_{ab}[RSH]\cdot[DIPEA]}{[DIPEAH^+]}}{k_{red}+k_{-}trans[Br]}} + \frac{k_{trans}\cdot\frac{\frac{k_{oxd}[I^*][ArBr]}{k_{trans}\cdot\frac{K_{ab}[RSH]\cdot[DIPEA]}{[DIPEAH^+]}}\cdot\frac{K_{ab}[RSH]\cdot[DIPEA]}{[DIPEAH^+]}}{k_{red}+k_{-}trans[Br]}}{k_{red}+k_{-}trans[Br]} \quad (11)$$

So:

$$[I\,*] = \frac{[Pd^*]total}{1+\frac{k_{oxd}[ArBr]}{k_{red}\cdot\frac{k_{trans}\cdot\frac{K_{ab}[RSH]\cdot[DIPEA]}{[DIPEAH^+]}}{k_{red}+k_{-}trans[Br]}}+\frac{k_{trans}\cdot\frac{\frac{k_{oxd}[ArBr]}{k_{trans}\cdot\frac{K_{ab}[RSH]\cdot[DIPEA]}{[DIPEAH^+]}}\cdot\frac{K_{ab}[RSH]\cdot[DIPEA]}{[DIPEAH^+]}}{k_{red}+k_{-}trans[Br]}}{k_{red}+k_{-}trans[Br]}} \quad (12)$$

Consequently the un-bridged steady state rate equation for the overall reaction should be:

$$rate = kred[III\,*] = koxd[I\,*][ArBr] = koxd\frac{[Pd^*]total}{1+\frac{k_{oxd}[ArBr]}{k_{red}\cdot\frac{k_{trans}\cdot\frac{K_{ab}[RSH]\cdot[DIPEA]}{[DIPEAH^+]}}{k_{red}+k_{-}trans[Br]}}+\frac{k_{trans}\cdot\frac{\frac{k_{oxd}[ArBr]}{k_{trans}\cdot\frac{K_{ab}[RSH]\cdot[DIPEA]}{[DIPEAH^+]}}\cdot\frac{K_{ab}[RSH]\cdot[DIPEA]}{[DIPEAH^+]}}{k_{red}+k_{-}trans[Br]}}{k_{red}+k_{-}trans[Br]}}\cdot[ArBr] \quad (1)$$

[27] Blackmond, D. G. *Angew. Chem. Int. Ed.* **2005**, *44*: 4302. For inductrial application of RPKA, see: Haddad, N.; Qu, B.; Lee, H.; Lorenz, J.; Varsolona, R.; Kapadia, S.; Sarvestani, M.; Feng, X.; Busacca, C.A.; Hebrault, D.; Rea, S.; Schellekens, L.; Senanayake, C.H. *Org. Process Res. Dev.* **2015**, *19*, 132.

[28] Shi, W.; Luo, Y.; Luo, X.; Chao, L.; Zhang, H.; Wang, J.; Lei, A. *J. Am. Chem. Soc.* **2008**, *130*, 14713.

[29] Inspection of the rate-law:

$$rate = \frac{d[III^*]}{dt} = koxd\frac{[Pd^*]total}{1+\frac{k_{oxd}\cdot[ArBr]}{k_{trans}\cdot\frac{K_{ab}[RSH]\cdot[DIPEA]}{[DIPEAH^+]}}+\frac{k_{oxd}[ArBr]}{k_{red}}}[ArBr] \quad (1')$$

Reveals that when k_{red} is far far smaller than k_{trans} and k_{oxd}, the third term in the denominator became the dominant term, the equation further reduced to:

$$rate = koxd\frac{[Pd^*]total}{1+\frac{k_{oxd}\cdot[ArBr]}{k_{trans}\cdot\frac{K_{ab}[RSH]\cdot[DIPEA]}{[DIPEAH^+]}}+\frac{k_{oxd}[ArBr]}{k_{red}}}\cdot[ArBr] = koxd\frac{[Pd^*]total}{\frac{k_{oxd}[ArBr]}{k_{red}}}\cdot[ArBr] = kred\cdot[Pd\,*]total \quad (13)$$

In other words, when reductive elimination is the rate-determining step, the overall reaction is zeroth order in both the bromide and the thiolate.

[30] The word "slow" is used in relative terms, compared to oxidative addition and transmetalation under current conditions. In absolute terms, the C–S reductive elimination is actually very fast, as all the reactions were completed within 10 min in the kinetic studies; Hartwig's kinetics work on C–S reductive elimination demonstrated that such process proceeded readily at temperature as low as 50 °C, see ref. 21.

[31] Novak and Grushin have established that Pd and P bond aryl exchange is highly dependent on the halide on Pd. For instance, the exchange in much more pronounced when I^- is on Pd than Br^-. Considering that pre-dissociation of one phosphine is required prior to exchange, this could be the result of trans effect. Since Br^- ranked was lower that sulfur in the trans effect hierarchy (Br^- <I^-<S), intermediate II in Figure 2 is not expected to be prone to undergo aryl exchange. Also note that aryl exchange is most severe when monodentate ligands like PPh_3 are used, see ref 20; such exchanges are suppressed by the employment of bidentate ligands.